RAPID COMMUNICATIONS

PHYSICAL REVIEW B VOLUME 46, NUMBER 11 15 SEPTEMBER 1992-I

# Scattering and spectral shape in ballistic-electron-emission microscopy of $NiSi_2$-Si(111) and Au-Si samples

H. D. Hallen,* A. Fernandez, T. Huang, J. Silcox, and R. A. Buhrman
*School of Applied and Engineering Physics, National Nanofabrication Facility and Materials Science Center, Cornell University, Ithaca, New York 14853-2501*
(Received 16 December 1991)

The ballistic-electron-emission microscopy (BEEM) tip voltage versus collector current spectral shape is used as a tool to study Au-Si and $NiSi_2$-Si samples on a nanometer scale. A method is outlined for the extraction of an energy-dependent transmission factor from the BEEM spectra. Results for Au-Si samples compare favorably with theoretical interface transmission calculations. Data from both systems suggest that the shape of the spectra is influenced by scattering. The influence of scattering induced broadening of the injected electron transverse momentum distribution is considered.

Ballistic-electron-emission microscopy (BEEM) has been shown to be a powerful tool for determining the Schottky barrier height (SBH) in several metal-semiconductor systems.[1,2] In the BEEM technique, electrons are injected by a scanning tunneling microscopy (STM) tip into a thin metal overlayer on a semiconductor. Those electrons which reach the buried interface are filtered with respect to energy and momentum by the Schottky interface. Within simple models of BEEM,[2] the near threshold functional form of the BEEM spectra (current traveling into the semiconductor versus sample to tip bias) can be understood and SBH's measured. In this paper we present a method to extract information about the transport of these electrons through the metal overlayer and across the buried interface. The method relies on changes in BEEM spectral shape both near and far from the threshold region. This represents the first attempt to use BEEM as a tool for studying transport and scattering processes with scannable nanometer resolution.

In their first two papers on BEEM, Kaiser and Bell proposed[1] and modified[2] a model to calculate the collector current versus voltage. We take this model as a starting point and add an arbitrary energy-dependent transport term[3] which, depending on the system under study, is dominated either by interface transport or scattering in the metal overlayer. We find that for the case of gold on silicon, the former is the most important unless the gold film has been strongly modified by stressing at high tunnel bias. After the stressing, defect-induced inelastic scattering effects dominate. Elastic scattering effects are observed in the silicide system.

The effect of energy dependent transport in a BEEM spectrum can be described by a function $H(E_x-E_{\min})=[1-s(E_x)]T(E_x-E_{\min})$, where $E_x$ is the kinetic energy normal to the interface, $s(E_x)$ is an energy-dependent scattering factor, and $T$ is the quantum-mechanical transmission factor for the interface. $E_{\min}$ is the minimum kinetic energy perpendicular to the interface required for transport into the semiconductor. Note that $E_x \sim E$ when elastic scattering effects are small as in the Au-Si system. The collector (BEEM) current $I_c$ is given by Eq. (5) of Ref. 2 with $H(E_x-E_{\min})$ inserted into the integral over $E_x$. This is converted to a matrix equation $\mathbf{I}_c=A\mathbf{H}$, where $A$ is known if a value for the SBH is given. The matrix $A$ is nearly singular due to the WKB factor $D(E_x)$. The inversion uses a singular value decomposition of the matrix $A$ (Ref. 4) with a minimum mean-square error choice of inverse singular values. A small magnitude low-frequency oscillation in $H$ is caused by the cutoff in the singular values.[5] The SBH is not known *a priori,* so an iterative procedure based on physical constraints on $H$ is used to obtain the correct SBH and the corresponding $H$. This method is more sensitive than a direct determination of SBH from the BEEM spectra threshold when $H$ is unknown.[6]

This method has been used to determine the device transmittance functions $H$ for both Au-Si [(100) and (111)] and epitaxial $NiSi_2$-Si(111) samples. The sample preparation has been described elsewhere.[5] Briefly, the silicide samples ~20–60 Å thick are produced under ultrahigh-vacuum (UHV) conditions and studied *in situ.* Au-Si sample preparation varied: 150 Å of gold was evaporated in a high vacuum of UHV after an aqueous hydrofluoric dip or hydrogen termination of the silicon surface in air or doping with oxygen or chlorine in UHV. Representative $H(E_x)$ are shown in Fig. 1. The data have been scaled so that they saturate at unity. This accounts for the unknown scaling factor $R$.[2] The function $H$ quantifies the deviation in shape from that calculated in the simple model of BEEM outlined in Ref. 2, which effectively assumes a constant $H$. In general, $H$ can reflect the quantum-mechanical interface transmission, energy-dependent scattering, or band-structure effects beyond the effective-mass approximation of the simple model.

First consider the spectra shown in Fig. 1(a) as circles. This is the most common BEEM spectral shape for Au-Si samples. In fact, to within the noise of the data, it is the only shape obtained away from special regions where the gold film has been stressed at a tunnel bias high enough ($\geq 2.5$ V) that changes could be seen in the local topography of the Au grains. Also shown in Fig. 1(a) is a solid line from a theoretical calculation of interface transmittance $T$ for the Au-Si(111) system.[7] The agreement is excellent, with no adjustable parameters, except for the low-frequency oscillations on $H$ produced by the inversion

 © 1992 The American Physical Society

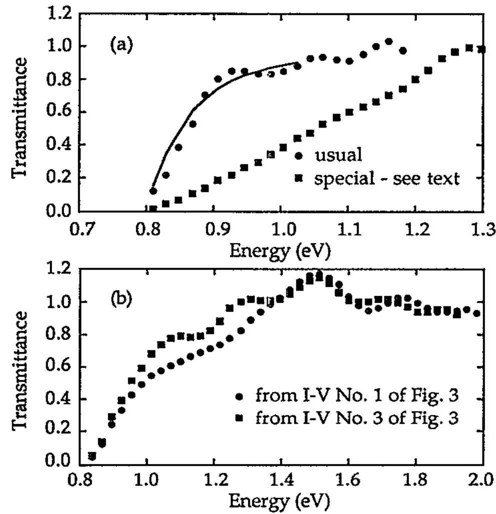


FIG. 1. Plot of experimental transmittance $H$ obtained from typical BEEM spectra of (a) Au-Si and (b) $B$-type $NiSi_2$-Si(111) samples with model parameters as in Ref. 11. The SBHs used are (a) 0.78 and 0.80 eV and (b) 0.84 and 0.86 eV for the circles and squares, respectively. The data are shifted to align the SBHs. The data are scaled by (a) 7.5 and 2.25 and (b) 8 and 12.8 for the circles and squares, respectively. Also shown in (a) is a theoretical calculation of $T(E_x)$ from Ref. 7.

process. This suggests that in the unmodified Au-Si system, the shape of the BEEM spectra is determined by the simple model with dynamic effects ($T$) included, i.e., there is no significant contribution from $s(E_x)$.

This is not the case for the data shown by the squares in Fig. 1(a) which do not reflect $T(E_x)$ for the interface, indicating that a nonconstant $s(E_x)$ is dominating the spectral shape. This slowly rising $H$ is found only where the gold film has been locally stressed by briefly raising the tip bias to high voltages. This suggests that inelastic scattering from the high density of induced point defects in the gold is responsible for the energy dependence of $s(E_x)$. This is supported by the observation that a variety of $H$ functions (for clarity, the figure shows only one example) are observed as opposed to a single $H$ as in unstressed regions, suggesting that $s(E_x)$ depends on the local character and density of defects in the modified Au.

Turning to the silicide data, a detailed calculation of the spectral shape in the $NiSi_2$-Si(111) cases has recently been given.[8] It takes into account the band structure of the $NiSi_2$, which in the simple BEEM model is approximated as a parabolic band, but does not include any scattering. The calculation shows a very low current immediately above the appropriate SBH, followed by a knee at about 1.4 V, above which $I_c$ rises sharply. The experimental BEEM spectra do not strongly reveal these features, generally exhibiting more current just above threshold than predicted by theory. To determine whether residual evidence of these band-structure features are present in the data, $H$ was calculated using the simple free-electron BEEM model.[2] While $H$ has no direct physical interpretation in this silicide case, the calculation of $H$ is still useful since differences in shape are much more evident in $H$ than in the $IV$ curve. Examples of the silicide data are shown in Fig. 1(b). $H$ from all the BEEM spectra on the silicides are similar, lying in a range near those in the figure. The difference between the silicide $H$'s and the minimal appearance of the theoretically predicted features [a rise near 1.3 V after a more flat region in the $H$ shown by the circles in Fig. 1(b)] can be explained by the existence of varying amounts of elastic scattering in the silicide layer. The variations in degree of scattering point to an extrinsic scattering mechanism. Even a little scattering upsets the strongly forward peaked momentum distribution of the electrons injected by the tip. The BEEM spectra then reflects averaging over a larger region of wave-vector space, smoothing the effects of band structure which dominate the results of the theoretical calculation. The amount of scattering required to account for the discrepancy can be roughly estimated by comparing the magnitude of the experimental spectra just above threshold to that of the theoretical calculation of Ref. 8 and another calculation which assumes an isotropic injected electron momentum distribution.[9] Isotropic point defect scattering of the order of 10% of the injected electrons appears to be sufficient to wash out the band-structure effects in this system. Thus while the experimental samples exhibit very good epitaxial interfaces and silicide layers, as revealed by cross-sectional transmission electron microscopy and high-resolution x-ray scattering,[10] the BEEM spectra is quite sensitive to a point defect density that is not readily revealed by such conventional analytical tools based on diffraction.

Stronger elastic scattering mechanisms which further broaden the injected electron distribution have other, very noticeable, effects on the BEEM data which are particularly evident at high bias when scaled BEEM spectra are compared. An example is shown in Figs. 2 and 3. Figure

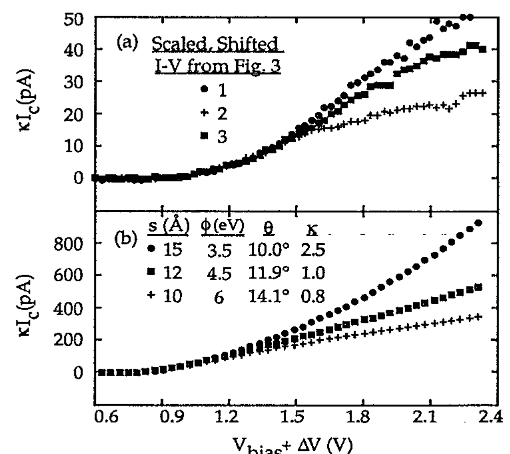


FIG. 2. (a) Illustrative single sweep BEEM spectra taken at 1 nA tunnel current are scaled by a factor $\kappa$ and shifted (see Table I) to coincide near threshold. (b) Scaled calculated BEEM spectra illustrate the effects of a change in the width of the injected electron momentum distribution (0.8 eV SBH). $s$, $\phi$, and $\theta$ are the tunnel distance, work function, and angle at which the distribution at 8 eV kinetic energy has dropped to $1/e$ its maximum value, respectively. The difference in current scale between (a) and (b) is due to inelastic scattering in the silicide and to interface transmittance effects.

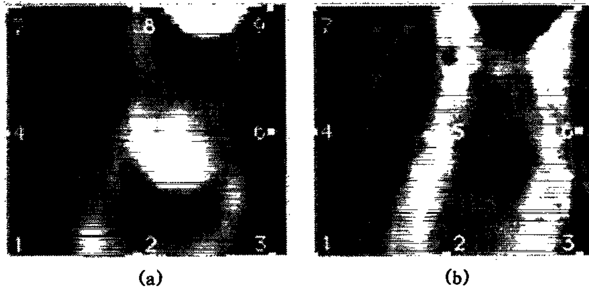

(a) (b)

FIG. 3. Gray scale 1.4 V, 1 nA constant current STM and BEEM images of a *B*-type $NiSi_2$-Si(111) sample. The images are 800×750 Å$^2$. Areas which are higher in topography or which have more BEEM current are shown with a lighter gray. (a) The STM topography with a gray range of 15 Å illustrating a misoriented grain (Ref. 10). The mounds are 8–25 Å tall and light gray regions 2–6 Å high. The left side of the scan is about 4 Å above the right. (b) The BEEM image. The 100-pA range makes the enhanced features (50–100 pA) whitish, and background features (20–30 pA) gray and (10–15 pA) dark gray. Marked on the images are the locations at which BEEM spectra were taken. Note the onset of BEEM current and topographic change are offset from each other. The spectra are compared in Table I and the other figures.

2(a) shows BEEM spectra shifted by a voltage $\Delta V$ and $I_c$ scaled by a factor $\kappa$ to coincide near threshold. A shape change is evident at higher voltages. This may be quantified by comparing the relative magnitudes of $\kappa I_c$ at 2.3 V (last row of Table I). The effect in the Figs. 2 and 3 case appears to be due to scattering of the injected tunnel electrons as they cross a buried grain boundary.[11] The different grains can be readily seen in the topographic image [Fig. 3(a)]. Associated with the grain boundary is contrast in the BEEM image. Most of the contrast is due to an overall energy-independent variation of $I_c$, as described in Ref. 11, but there is also a significant change in the shape in the spectra, which is of interest here. The changes in shape seen in Fig. 2(a) are directly attributable to a strongly broadened electron momentum distribution. This can be demonstrated and the amount of broadening estimated by considering a theoretical calculation of BEEM spectra using a model similar to the simple model[2,12] where the calculated width of the tunnel electron momentum distribution is altered through the artifice of changing the effective work function $\phi$ and tunnel distance $s$ used in the calculation. The model has been modified to account for the band minimum offset from zero transverse wave vector of the Si(111) interface by allowing transport into an annulus of transverse wave vectors, and multiplying by an energy-dependent factor to account for the fraction of the annulus occupied by the conduction-band minima.[11] The calculated tunnel current constrains the relative values of $\phi$ and $s$. The resulting scaled spectra of Fig. 2(b) indicate that an energy-independent broadening of the momentum distribution can describe the phenomenon. Since an overall, energy-independent increase in $I_c$ and a shape change at higher bias are both caused by a broader injected electron distribution, it is tempting to compare amplitude and shape of all BEEM spectra. This is not always valid since there are mechanisms, e.g., strong elastic scattering, which can effect the amplitude without necessarily changing the shape. Nevertheless, we do find some correlation between BEEM spectral shape at high voltages (Fig. 2) and $I_c$ amplitude within a scan (e.g., Fig. 3, Table I). In contrast, the small differences in shape at lower bias evident in $H$ [Fig. 1(b)] do not obviously correlate with $\kappa$, presumably because they are lost with only a comparably small amount of elastic scattering.

We have shown that the shape of the BEEM spectra can give information about the interface transmittance $T$, or about elastic and inelastic scattering from defects in the sample, particularly when supported by theoretical calculations of the ideal transmittance. To gain a better understanding of the BEEM process it is also important to note some of the properties to which the spectra are not sensitive. We find that the BEEM spectral shape is independent of the silicon face in the Au-Si(111) or (100) systems, and explain this fact in terms of a relaxation in the transverse momentum constraints. The shape of the BEEM spectra is also independent of interfacial chemistry and cleanliness in the Au-Si system. This is evidenced by identical $H$ found for samples with monolayers of oxide, chlorine, hydrogen, or hydrocarbons at the interface. Neither is the spectral shape changed by Au-Si *interface* modification.[5] Some variation in apparent SBH (threshold voltage $V_T$) is seen on all samples. High-quality interfaces are expected to have uniform SBH; but a variation in $V_T$, typically tens of millivolts, is omnipresent in both systems. A much larger ~100 mV variation is sometimes found in the Au-Si system, but this latter seems to be directly related to a high defect density arising from a structure modification, and is only seen in conjunction with odd-shaped $H$ such as that in Fig. 1(a). We suggest the more common small scale variation in $V_T$ could be the

TABLE I. The relative scaling factors $\kappa$ and threshold shifts $\Delta V$ needed to align the spectra near the threshold region. Also shown are the relative magnitude (Rel. Mag.) of the scaled BEEM current $\kappa I_c$ at 2.3 V [see Fig. 2(a)]. The latter variation results from differences in spectral shape which are correlated with differences in the silicide microstructure. The first BEEM spectra has arbitrarily been chosen as the standard.

| | Spectra No. | | | | | | | | |
|---|---|---|---|---|---|---|---|---|---|
| | 1 | 2 | 3 | 4 | 5 | 6 | 7 | 8 | 9 |
| $\kappa$ | 1.0 | 0.65 | 1.15 | 1.0 | 0.45 | 1.15 | 1.2 | 0.31 | 0.65 |
| $\Delta V$ | 0.0 | −0.03 | 0.02 | 0.0 | −0.03 | 0.03 | 0.0 | 0.04 | 0.04 |
| Rel. Mag. | 1.0 | 0.4 | 0.72 | 0.9 | 0.7 | 0.8 | 1.2 | 0.67 | 0.67 |

remnant signature of a major variation in interface dipoles, which are not resolved by BEEM due to compensating fields within the Si.[13] The value of the $V_T$ is correlated spatially with grains, as can be seen in Fig. 3 and Table I. Of interest here is that the small scale variation in $V_T$ does not affect the shape of the BEEM spectra in either the epitaxial or nonepitaxial systems.

In summary, we have studied the shape of the BEEM spectra of Au-Si and $NiSi_2Si$ samples in an effort to discover its sensitivity to transport properties of the metal base. We find that interface transmission effects dominate $H$ on unstressed areas of Au-Si samples. Hence we are able to measure interface transmission functions and compare to theory. Strong elastic scattering that is created in local regions of the metal base layer by briefly applying a high tip bias results in changes of BEEM spectral shape and scaling. In the epitaxial silicide case, the shape of $H$ is very sensitive to a small amount of scattering; stronger elastic scattering produces changes in scaling and spectral shape at higher voltage. A model calculation illustrates the effect of broadening the injected electron momentum distribution on the shape of the BEEM spectra. Processes which change the scaling of the BEEM spectra or shift $V_T$ leaving the shape intact are noted. If shape, threshold position and scaling are used, one can use the scanning ability of an STM in BEEM mode to effectively study details of electron transport on a nanometer scale.

During part of the time this work was done, H.D.H. was supported by IBM, and A.F. by the Hertz Foundation. Research support was provided by the Office of Naval Research and the Semiconductor Research Corporation. This research project also received initial support from the National Nanofabrication Facility and the Cornell Materials Science Center, which are supported by the National Science Foundation.

*Present address: 1D-204 AT&T Bell Laboratories, 600 Mountain Avenue, Murray Hill, NJ 07974.

[1]W. J. Kaiser and L. D. Bell, Phys. Rev. Lett. **60**, 1406 (1988).

[2]L. D. Bell and W. J. Kaiser, Phys. Rev. Lett. **61**, 2368 (1988).

[3]M. Prietsch and R. Ludeke, Phys. Rev. Lett. **66**, 2511 (1991), inserted a fixed functional form to account for interface transmission effects ($T$).

[4]Gene H. Golub and Charles F. Van Loan, *Matrix Computations* (Johns Hopkins Univ. Press, Baltimore, MD, 1987); William H. Press *et al.*, *Numerical Recipes* (Cambridge Univ. Press, Cambridge, 1986).

[5]H. D. Hallen, Ph.D. thesis, Cornell University, 1991 (unpublished).

[6]The sensitivity depends on how accurately one can apply the constraint that $H$ begins to rise at the SBH without a nonphysical spike (~0.03 eV for the Au-Si case and ~0.05 eV for the silicide $H$).

[7]E. Y. Lee and L. J. Schowalter, J. Appl. Phys. **65**, 4903 (1989).

[8]M. D. Stiles and D. R. Hamann, Phys. Rev. Lett. **66**, 3179 (1991).

[9]M. D. Stiles (private communication).

[10]J. Brock (private communication).

[11]A. Fernandez, H. D. Hallen, T. Huang, R. A. Buhrman, and J. Silcox, Phys. Rev. B **44**, 3428 (1991).

[12]Parameters used in the theoretical model are discussed in Ref. 5. A tunnel distance of 11 Å, effective mass 0.3, and work function of 4 eV are used.

[13]J. L. Freeouf *et al.*, Appl. Phys. Lett. **40**, 634 (1982); J. Vac. Sci. Technol. **21**, 570 (1982).